SCIENTIFIC REPORTS

OPEN

SUBJECT AREAS:
NANOPHOTONICS AND PLASMONICS
SUB-WAVELENGTH OPTICS

Received
22 September 2014

Accepted
30 October 2014

Published
20 November 2014

Correspondence and requests for materials should be addressed to J.W.Y. (jaeyoon@uta.edu)

Ultrahigh-Q metallic nanocavity resonances with externally-amplified intracavity feedback

Jae Woong Yoon[1], Seok Ho Song[2] & Robert Magnusson[1]

[1]Dept. of Electrical Engineering, University of Texas - Arlington, Box 19016, Arlington, TX 76019, USA, [2]Dept. of Physics, Hanyang University, Seoul 133-791, KOREA.

We propose a mechanism of ultrahigh-Q metallic nanocavity resonances that involves an efficient loss-compensation scheme favorable for room-temperature operation. We theoretically show that surface plasmon-polaritons excited on the entrance and exit interfaces of a metallic nanocavity array efficiently transfer external optical gain to the cavity modes by inducing resonantly-amplified intracavity feedback. Surprisingly, the modal gain in the nanocavity with the externally amplified feedback is inversely proportional to the cavity length as opposed to conventional optical cavity amplifiers requiring longer cavities for higher optical gain. Utilizing this effect, we numerically demonstrate room-temperature nanocavity resonance Q-factor exceeding 10^4 in a 25-nm-wide silver nanoslit array. The proposed mechanism provides a highly efficient plasmonic amplification process particularly for subwavelength plasmonic cavities which are essential components in active nanoplasmonic devices.

To develop advanced optical elements requiring small feature dimensions and innovative light-interaction schemes, plasmonic nanosystems are of immense interest because of their unique deep-subwavelength light localization properties and associated strong field enhancement. These attributes potentially enable various applications such as optical sensors[1], light absorbers[2], metamaterials[3–5], and nonlinear optical devices[6]. Among the many challenges in converting these properties to practice in device engineering is achieving high-Q plasmonic resonances in real metallic nanosystems that generally possess large ohmic absorption.

Considerable research has been devoted to establishing high-Q resonances in various metallic structures. In the classical attenuated total reflection configurations, the surface plasmon-polariton (SPP) resonance Q-factor is normally on the order of ~ 10–10^2 in the visible spectral domain[7]. In more advanced geometries such as metal-coated whispering gallery microcavities[8–11], the resonance Q-factor approaches $\sim 10^4$. Despite the modest resonance Q-factors associated with plasmonic resonators as compared to those exceeding 10^8 in photonic microcavities[12,13], high-Q plasmonic resonators are under extensive investigation due to their deep-subwavelength localization properties. In addition to the potential for high-density optical integration, plasmonic nanocavities may enable quantum optical devices that take advantage of large Purcell enhancement and strong cavity QED coupling[14–16]. Achieving large figure-of-merit (FOM) $\lambda^3 Q/D^3$ is important in this context; here λ is the vacuum wavelength and D is the feature dimension of the resonant mode. Recent theoretical analyses show low-temperature FOM $\sim 10^9$ and extremely large Purcell enhancement factor $\sim 10^5$ in various types of plasmonic nanocavities[17–19] with $D \sim \lambda/10$. However, plasmonic modes in metallic nanocavities have inherently large ohmic damping that scales with $1/D$, resulting in substantially limited FOM at room temperature. Recovering high FOM by gain-assisted loss compensation is presently believed to be difficult because of strong fluorescence quenching caused by lossy surface wave excitations[20,21]. Therefore, most of the previous work on loss compensation in plasmonic nanocavities has been performed at low operating temperatures since the optical gain required for room-temperature operation is unrealistically large.

In this paper, we propose a new mechanism of ultrahigh-Q metallic nanocavity resonances assisted by amplified cavity-boundary feedback. We show that SPPs at the entrance and exit interfaces of a nanocavity array can be used as carriers of external optical gain furnished to the plasmonic modes inside metallic nanocavities. Notably, the SPP-mediated optical gain transfer to the nanocavity provides a promising loss-compensation channel that is favorable for room-temperature operation of narrow nanocavity resonances with moderate optical gain. This loss-compensation channel allows the nanocavity mode to obtain dominant modal gain by the externally amplified feedback from the interfacial SPPs rather than the direct stimulated emission inside the

nanocavity. In contrast to conventional optical cavity amplifiers that require a longer cavity length for larger modal gain, the nanocavity gain due to the externally amplified feedback is inversely proportional to the cavity length. We theoretically demonstrate a room-temperature resonance Q-factor exceeding 10^4 for a plasmonic nanocavity mode with feature size $D \sim \lambda/30$ in a metallic nanoslit array surrounded by an external gain medium with a moderate gain constant.

Metallic nanocavities under the influence of a gain-assisted interfacial Fano resonance

We consider plasmonic nanocavity resonances in a periodic array of deep-subwavelength metallic nanoslits as schematically depicted in Fig. 1. An incident transverse-magnetic planewave at the entrance interface couples to a fundamental cavity mode (CM) with the single-interface transmission coefficient τ. For deep-subwavelength slits, the excited CM generally has a fairly high internal reflection coefficient ρ_{in} because of the large impedance mismatch between the unbound external wave and CM with tight lateral confinement. Therefore, the excited CM induces characteristic Fabry-Pérot-like resonances[22–25] when a constructive interference occurs at the phase-matching condition

$$\beta' L = (q+1)\pi - \arg(\rho_{in}), \qquad (1)$$

where L is the thickness of the metal film or cavity length equivalently, β' is real part of the complex propagation constant of the CM, and the integer q is Fabry-Pérot order corresponding to the number of longitudinal nodes inside the cavity.

According to our recent analysis[26], surface plasmon-polaritons (SPP) at the entrance and exit interfaces cause interfacial Fano resonances that drastically modify τ and ρ_{in} within their resonance bandwidth. The effects of the SPP-mediated interfacial Fano resonance include the antiresonant extinction of τ, i.e., $\tau \to 0$, and associated total internal reflection of the CM, i.e., $|\rho_{in}| \to 1$. This antiresonance effect causes non-radiative CM resonances with extremely high-Q factors. For real metals at room temperature, high ohmic absorption strongly suppresses this resonance.

The purpose of this paper is to demonstrate the possibility of ultrahigh-Q plasmonic nanocavity resonances at the SPP-induced antiresonance condition with an appropriate loss compensation method. Plasmonic amplification or SPASER oscillation in metallic nanocavities is generally challenging due to the high loss of the plasmonic modes and strong fluorescence quenching of the emitters in the nanometric vicinity of metal surfaces[20,21]. In this aspect, loss compensation of the resonance with the total internal reflection due to the interfacial SPPs provides an amplification channel via the external gain medium that avoids the fluorescence quenching effect inside the nanoslit.

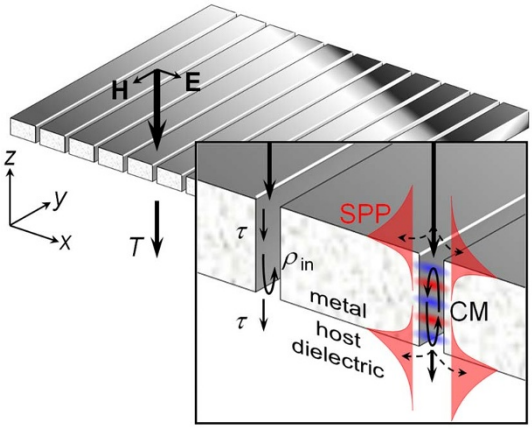

Figure 1 | Schematic of a metallic nanoslit array with resonant SPP and CM excitations. Coupling of external light with the fundamental CM is described by the single-interface transmission τ and internal reflection ρ_{in} coefficients, respectively. SPPs at the entrance and exit interfaces lead to resonant behavior of τ and ρ_{in} that drastically modify CM resonance properties inside the slits.

We now theoretically demonstrate a gain-assisted ultrahigh-Q CM resonance near the antiresonance condition. We consider an Ag nanoslit array imbedded in a host dielectric with optical gain. We use the finite element method[27] (FEM) and rigorous coupled-wave analysis[28] (RCWA) for our numerical study. We assume the realistic $\varepsilon_M = \varepsilon_M' + i\varepsilon_M''$ of Ag experimentally obtained by Johnson and Christy[29] and the host dielectric material is modeled by a complex refractive index $1.5 + ik$, where $k < 0$ adjusts the amount of optical gain.

We first find the response of an isolated surface of an Ag nanoslit array in the absence of optical gain. Figure 2(a) shows the spectral profiles of the single-interface transmittance $|\tau|^2$ and surface-excitation intensity $|E_z|^2$ averaged over a period at the Ag-dielectric interface for a semi-infinite array depicted in the inset. These single-interface responses are calculated using FEM. The single Lorentzian peak centered at wavelength $\lambda = 715$ nm in the surface excitation spectrum and the associated Fano profile in the single-interface transmittance spectrum confirm the SPP-induced Fano resonance at the Ag-dielectric interface.

This interfacial Fano resonance profile in the $|\tau|^2$ spectrum has its enhanced maximum at $\lambda = 700$ nm and antiresonant extinction at $\lambda = \lambda_{AR} = 745$ nm. For an Ag nanoslit array with the identical slit width and period but finite thickness, a high-Q nanocavity resonance is expected near λ_{AR} where the total internal reflection occurs. Figure 2(b) shows the film-transmittance (T) spectrum for Ag-film thickness $L = 460$ nm with no optical gain ($k = 0$) in the dielectric host. This film-transmittance spectrum is calculated using RCWA. Three major CM resonance peaks appear at wavelengths 644.5 nm, 706.0 nm, and 877.5 nm for Fabry-Pérot resonance orders $q = 5$, 4, and 2, respectively. The CM resonance peak for $q = 3$ at wavelength 740.5 nm is under the effect of the antiresonance condition and is missing in the T spectrum because of the high loss-sensitivity of a high-Q CM resonance. A more detailed explanation of the CM resonance under the influence of the SPP-induced antiresonance condition in the presence of material dissipation is provided in [26].

We apply a realistic amount of optical gain in the top and bottom dielectric layers and assume no gain inside the nanoslit cavities. The optical gain is described by the negative imaginary part $k = -2.26 \times 10^{-3}$ of the dielectric film's refractive index. This value corresponds to an optical gain constant 192 cm^{-1} at $\lambda = 740.5$ nm and is experimentally obtainable in dye-doped poly(methyl methacrylate)[30] (PMMA) with moderate doping concentration $\sim 10^{19}$ cm^{-3} and pumping density ~ 10 mJ/cm^2. Taking a small signal approximation that is reasonable for a low-intensity response of a gain medium under the lasing threshold[31,32], we calculate the T spectrum using RCWA; the result is shown in Fig. 2(c). We confirm an extremely narrow bandwidth ~ 44 pm (FWHM) and a high resonance Q-factor $\sim 1.7 \times 10^4$ of the CM resonance peak for $q = 3$. At the peak wavelength, the electric field intensity enhancement factor $|E/E_0|^2$ inside the 25-nm-wide nanoslit exceeds 3.6×10^4 as shown in the inset of Fig. 2(c).

The gain-assisted CM resonance in Fig. 2(c) is not simply understood by a direct stimulated emission to the CM because the optical gain region is external to the nanoslit cavities. Moreover, the assumed gain constant 192 cm^{-1} is far smaller than the attenuation constant $\beta'' = 630.5$ cm^{-1} of the CM. The β'' value is given by the dispersion equation[33]

$$\varepsilon_M \tanh\left[w\left(\beta^2 - k_0^2\right)^{1/2}/2\right] = -\left[\left(\beta^2 - \varepsilon_M k_0^2\right)/\left(\beta^2 - k_0^2\right)\right]^{1/2} \qquad (2)$$

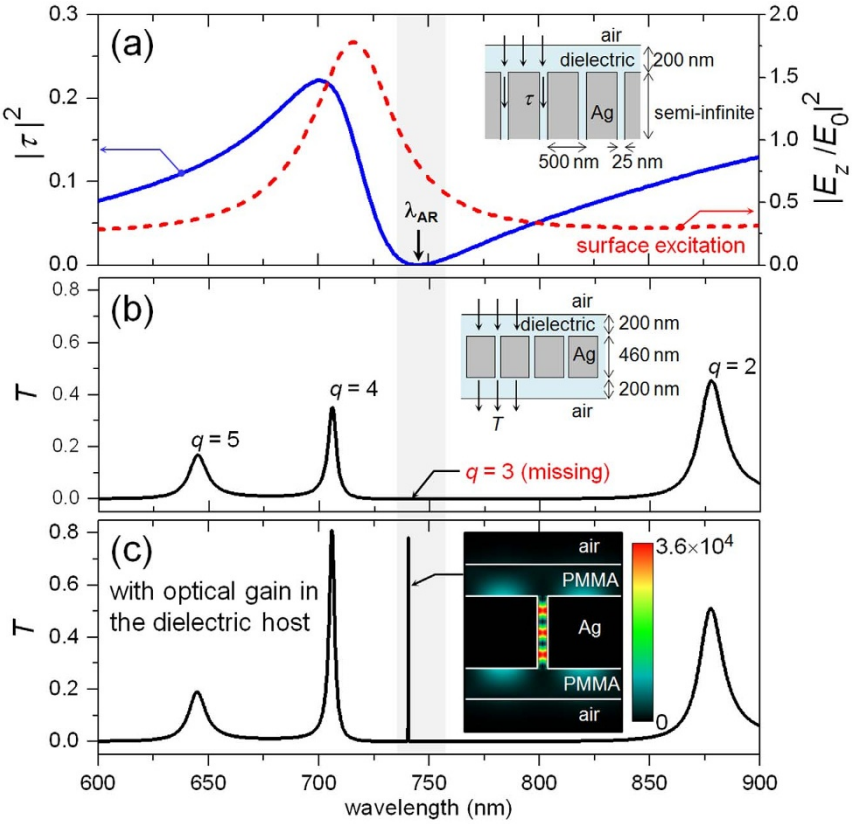

Figure 2 | Ultrahigh-Q nanocavity resonance by loss compensation with experimentally realistic level of optical gain in the surrounding dielectric. (a) Single interface transmittance $|\tau|^2$ (blue solid curve) and average surface excitation $|E_z/E_0|^2$ (red dotted curve) spectra with no optical gain ($k = 0$) in the dielectric host. Film-transmittance T for Ag film thickness $L = 460$ nm is shown in (b) for no optical gain ($k = 0$) and in (c) for optical gain of $k = -2.26 \times 10^{-3}$. The inset color-density plot in (c) shows electric field intensity $|E/E_0|^2$ (E_0: incident electric field) at the CM resonance peak for $q = 3$.

at $\lambda = 740.5$ nm for the case in Fig. 2(c), where $\beta = \beta' + i\beta''$ is the complex propagation constant of the CM, $k_0 = 2\pi/\lambda$ is the vacuum wave number and w is the slit width.

Externally amplified intracavity feedback

To understand this seemingly counter-intuitive result, we further analyze the response of the SPP-resonant surface of the Ag nanoslit array in the presence of optical gain in the host dielectric medium. Thus, we estimate the attenuation α_{SPP} and gain Γ_{SPP} constants of the SPP at the Ag-dielectric interface. We calculate the surface excitation $|E_z|^2$ spectrum of a semi-infinite Ag nanoslit array as a function of absorption factor $0 \leq f_{abs} \leq 1$ that controls the amount of ohmic absorption in Ag with its dielectric constant $\varepsilon_M = \varepsilon_M' + if_{abs}\varepsilon_M''$. In real experiment, adjusting f_{abs} corresponds to temperature tuning such that $f_{abs} = 1$ at room temperature and $f_{abs} < 1$ in the lower temperature range[34]. Figure 3(a) shows the result for $f_{abs} = 0.2$, 0.4, 0.6, 0.8, and 1.0 with no optical gain ($k = 0$) in the host dielectric. The bandwidth of the surface excitation spectrum indicates the total decay constant of the SPP. Figure 3(b) shows the measured half-width at half-maximum (HWHM), i.e., total decay constant γ_{tot} of the surface excitation spectrum, as a function of f_{abs}. The total decay constant at $f_{abs} = 0$, $\gamma_{tot}(f_{abs} = 0)$, represents the radiation decay constant γ_{rad} and thereby the attenuation constant α_{SPP} at $f_{abs} = 1$ is given by $\alpha_{SPP} = \gamma_{tot}(f_{abs} = 1) - \gamma_{tot}(f_{abs} = 0)$. This method to estimate α_{SPP} is valid for the small modal attenuation regime[34] where γ_{tot} is a linear function of f_{abs}. Figure 3(b) shows the linear dependence of γ_{tot} on f_{abs} and thus justifies the method to estimate α_{SPP} in our case. We obtain $\alpha_{SPP} = 53.7$ cm^{-1} as indicated in Fig. 3(b). The gain constant Γ_{SPP} is obtained by the difference between the HWHM values for $k = 0$ and $k = -2.26 \times 10^{-3}$ at $f_{abs} = 1$. The surface excitation spectrum for $k = -2.26 \times 10^{-3}$ at $f_{abs} = 1$ is indicated by black curve in Fig. 3(a), and its HWHM is indicated by the blue dotted horizontal line in Fig. 3(b). We obtain $\Gamma_{SPP} = 152.1$ cm^{-1}. As a result, we confirm a positive net modal gain of $\Gamma_{SPP} - \alpha_{SPP} = 98.4$ cm^{-1} of the SPP for the Ag nanoslit array considered in Fig. 2.

The response of the SPP-resonant surface in the presence of optical gain suggests that the dominant loss-compensation channel is the externally-amplified internal reflection (ρ_{in}) provided by the SPP at the interface as no optical gain is assumed inside the nanoslits. Thus, the amplified SPP yields the amplified internal reflectance $|\rho_{in}|^2 > 1$ at the SPP-mediated antiresonance condition. Using the FEM, we calculate the single-interface transmittance $|\tau|^2$ and internal reflectance $|\rho_{in}|^2$ for $k = 0$ and -2.26×10^{-3}. Figure 4 shows the results. We confirm amplified internal reflectance $|\rho_{in}|^2 > 1$ over the wavelength range from 719 nm to 772 nm. In particular, $|\rho_{in}|^2 = 1.0595$ at wavelength 740.5 nm corresponding to the high-Q CM resonance peak in Fig. 2(c). This internal reflectance value leads to an effective modal gain $\Gamma_{SPP\text{-}to\text{-}CM} = \ln|\rho_{in}|/L = 628.2$ cm^{-1} to the CM inside the nanoslit. With this optical gain from the amplified internal reflection, the high-Q CM resonance is obtained with a negligibly small net attenuation of the CM $\alpha_{net} = \beta'' - \Gamma_{SPP\text{-}to\text{-}CM} = 2.3$ cm^{-1}. Note that the attenuation constant $\beta'' = 630.5$ cm^{-1} without the SPP-induced interfacial amplification. Importantly, the optical gain $\Gamma_{SPP\text{-}to\text{-}CM} = \ln|\rho_{in}|/L$ transferred from the SPP to the CM is inversely proportional to the cavity length L because the number of internal reflections per unit optical path length is inversely proportional to L. Therefore, the SPP-induced antiresonance effect provides a mechanism for generating strong optical fields particularly in short cavities.

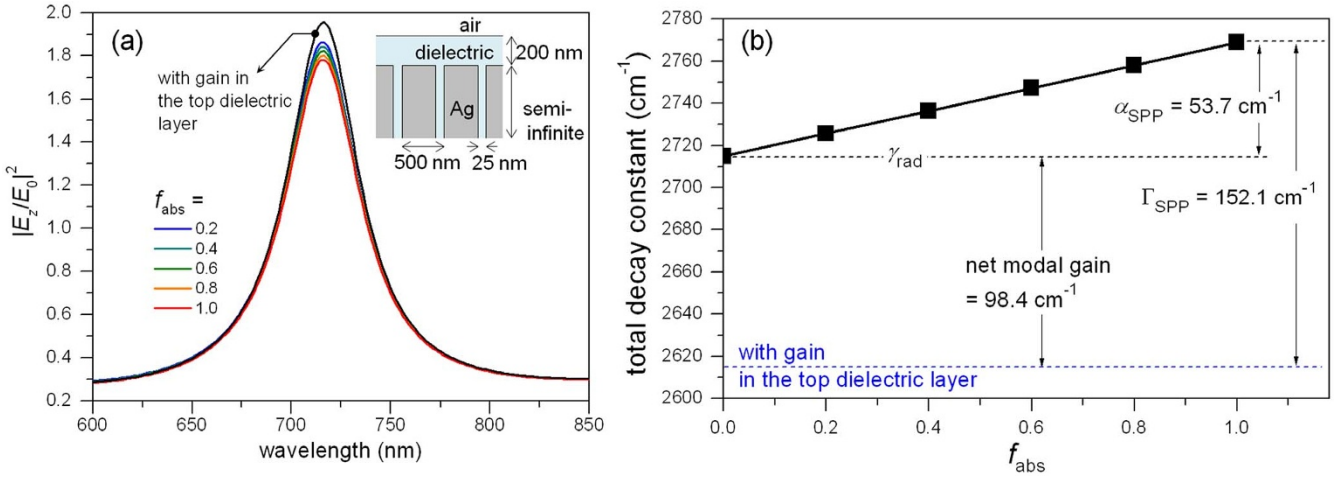

Figure 3 | Gain-assisted properties of an SPP on an Ag slit array. (a) Surface excitation $|E_z/E_0|^2$ spectra for different absorption factor f_{abs} and gain in the top dielectric layer. The black curve represents $f_{abs} = 1$ and the top dielectric layer with optical gain given by negative imaginary refractive index $k = -2.26 \times 10^{-3}$. No optical gain ($k = 0$) in the top dielectric layer is assumed in the spectra for $f_{abs} = 0.2$ (blue), 0.4 (cyan), 0.6 (green), 0.8 (orange), and 1.0 (red). (b) Estimated modal attenuation and gain constants of the SPP. The square symbols represent half-width at half-maximum (HWHM) of the surface excitation spectra in (a) as a function of f_{abs}, and the blue dotted horizontal line indicates HWHM for the top PMMA with optical gain.

Conclusions

In conclusion, we propose a new ultrahigh-Q nanocavity resonance mechanism pertinent to metallic nanoslit arrays. The SPP-induced antiresonant extinction condition leads to non-radiative resonances providing an efficient loss compensation channel based on externally-amplified interfacial feedback. Assuming a 25-nm-wide Ag nanoslit array imbedded in a dye-doped polymer film under realistic optical pumping density, we theoretically demonstrated an ultrahigh-Q plasmonic nanocavity resonance with resonance Q-factor exceeding 10^4. Considering further experimental study, the proposed device architecture with high aspect ratio nanoslits can be fabricated preferably by metallization of a lamellar dielectric grating structure[35,36] as this method does not demand challenging deep anisotropic etch through a metallic film to define nanoscale slits. It is of great interest to apply the proposed nanocavity feedback mechanism to various plasmonic nanosystems for ultra-small plasmonic lasers, efficient quantum-plasmonic elements, and compact nonlinear optical templates.

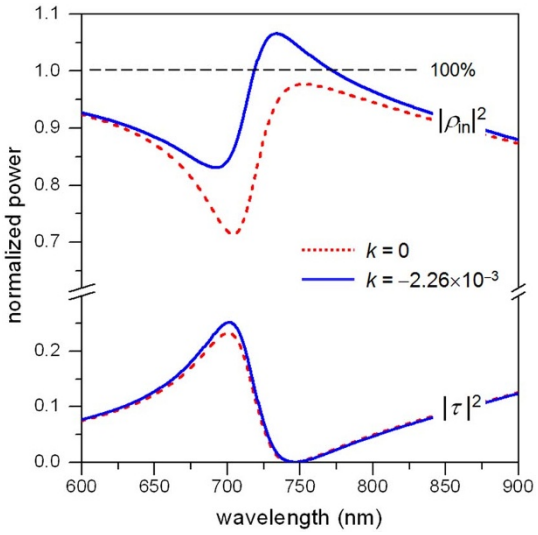

Figure 4 | Gain-assisted responses of an SPP-resonant Ag slit interface. The single-interface transmittance $|\tau|^2$ and internal reflectance $|\rho_{in}|^2$ of the SPP-resonant Ag nanoslit array with (blue solid curve) and without (red dotted curve) optical gain in the host dielectric material.

1. Wu, C. *et al.* Fano-resonant asymmetric metamaterials for ultrasensitive spectroscopy and identification of molecular monolayers. *Nat. Mater.* **11**, 69–75 (2012).
2. Teprik, T. V. *et al.* Omnidirectional absorption in nanostructured metal surfaces. *Nat. Photonics* **2**, 299–301 (2008).
3. Valentine, J. *et al.* Three-dimensional optical metamaterial with a negative refractive index. *Nature* **455**, 376–379 (2008).
4. Choi, M. *et al.* A terahertz metamaterial with unnaturally high refractive index. *Nature* **470**, 369–373 (2011).
5. Cai, W., Chettiar, U. K., Kildishev, A. V. & Shalaev, V. M. Optical cloaking with metamaterials. *Nat. Photonics* **1**, 224–227 (2007).
6. Linden, S. *et al.* Collective effects in second-harmonic generation from split-ring-resonator arrays. *Phys. Rev. Lett.* **109**, 015502 (2012).
7. Homola, J., Yee, S. S. & Gauglitz, G. Surface plasmon resonance sensors: review. *Sens. Actuator B-Chem.* **54**, 3–15 (1999).
8. Min, B. *et al.* High-Q surface-plasmon-polariton whispering-gallery microcavity. *Nature* **457**, 455–458 (2009).
9. Xiao, Y.-F. *et al.* High-Q exterior whispering-gallery modes in a metal-coated microresonator. *Phys. Rev. Lett.* **105**, 153902 (2010).
10. Chen, Y.-H. & Guo, L. J. High Q long-range surface plasmon polariton modes in sub-wavelength metallic microdisk cavity. *Plasmonics* **6**, 183–188; DOI:10.1007/s11468-010-9185-0 (2011).
11. Rottler, A. *et al.* High-Q hybrid plasmon-photon modes in a bottle resonator realized with a silver-coated glass fiber with a varying diameter. *Phys. Rev. Lett.* **111**, 253901 (2013).
12. Armani, D. K., Kippenberg, T. J., Spillane, S. M. & Vahala, K. J. Ultra-high-Q toroid microcavity on a chip. *Nature* **421**, 925–928 (2003).
13. Lee, H. *et al.* Chemically etched ultrahigh-Q wedge-resonator on a silicon chip. *Nat. Photonics* **6**, 369–373 (2012).
14. Gong, Y. Y. & Vučković, J. Design of plasmon cavities for solid-state cavity quantum electrodynamics applications. *Appl. Phys. Lett.* **90**, 033113 (2007).
15. Akimov, A. V. *et al.* Generation of single optical plasmons in metallic nanowires coupled to quantum dots. *Nature* **450**, 402–406 (2007).
16. de Leon, N. P., Lukin, M. D. & Park, H. Quantum plasmonic circuits. *IEEE J. Sel. Top. Quantum Electron.* **18**, 1781–1791 (2012).
17. Seo, M.-K., Kwon, S.-H., Ee, H.-S. & Park, H.-G. Full three-dimensional subwavelength high-Q surface-plasmon-polariton cavity. *Nano Lett.* **9**, 4078–4082 (2009).
18. Kang, J.-H., No, Y.-S., Kwon, S.-H. & Park, H.-G. Ultrasmall subwavelength nanorod plasmonic cavity. *Opt. Lett.* **36**, 2011–2013 (2011).
19. Kwon, S.-H. Deep subwavelength plasmonic whispering-gallery-mode cavity. *Opt. Express* **20**, 24918–24924; DOI:10.1364/OE.20.024918 (2012).
20. Barnes, W. L. Fluorescence near interfaces: the role of photonic mode density. *J. Mod. Opt.* **45**, 661–699 (1998).
21. Dulkeith, E. *et al.* Fluorescence quenching of dye molecules near gold nanoparticles: radiative and nonradiative effects. *Phys. Rev. Lett.* **89**, 203002 (2002).

22. Porto, J. A., García-Vidal, F. J. & Pendry, J. B. Transmission resonances on metallic gratings with very narrow slits. *Phys. Rev. Lett.* **83**, 2845–2848 (1999).
23. Ding, Y., Yoon, J., Javed, M. H., Song, S. H. & Magnusson, R. Mapping surface-plasmon polaritons and cavity modes in extraordinary optical transmission. *IEEE Photon. J.* **3**, 365–374; DOI:10.1109/JPHOT.2011.2138122 (2011).
24. Sturman, B. & Podivilov, E. Theory of extraordinary light transmission through arrays of subwavelength slits. *Phys. Rev. B* **77**, 075106 (2008).
25. Yoon, J. W., Jung, M. J., Song, S. H. & Magnusson, R. Analytic theory of the resonance properties of metallic nanoslit arrays. *IEEE J. Quantum Electron.* **48**, 852–861 (2012).
26. Yoon, J. W., Lee, J. H., Song, S. H. & Magnusson, R. Unified theory of surface-plasmonic enhancement and extinction of light transmission through metallic nanoslit arrays. *Sci. Rep.* **4**, 5683; DOI:10.1038/srep05683 (2014).
27. Jin, J. *The finite element method in electromagnetic*. 2nd Ed. New York: John Wiley and Sons (2002).
28. Moharam, M. G. & Gaylord, T. K. Rigorous coupled-wave analysis of planar-grating diffraction. *J. Opt. Soc. Amer.* **71**, 811–818 (1981).
29. Johnson, P. B. & Christy, R. W. Optical constants of the noble metals. *Phys. Rev. B* **6**, 4370–4379 (1972).
30. Noginov, M. A. *et al.* Stimulated emission of surface plasmon polaritons. *Phys. Rev. Lett.* **101**, 226806 (2008).
31. Avrusky, I. Surface plasmons at nanoscale relief gratings between a metal and a dielectric medium with optical gain. *Phys. Rev. B* **70**, 155416 (2004).
32. Noginov, M. A. *et al.* Compensation of loss in propagating surface plasmon polariton by gain in adjacent dielectric medium. *Opt. Express* **16**, 1385–1392; DOI:10.1364/OE.16.001385 (2008).
33. Dionne, J. A., Sweatlock, L. A. & Atwater, H. A. Plasmon slot waveguides: Towards chip-scale propagation with subwavelength-scale localization. *Phys. Rev. B* **73**, 035407 (2006).
34. Yoon, J., Song, S. H. & Kim, J.-H. Extraction efficiency of highly confined surface plasmon-polaritons to far-field radiation: an upper limit. *Opt. Express* **16**, 1269–1279; DOI:10.1364/OE.16.001269 (2008).
35. García-Vidal, F. J. *et al.* Localized surface plasmons in lamellar metallic gratings. *J. Lightwave Technol.* **17**, 2191–2195 (1999).
36. Collin, S. *et al.* Nearly perfect Fano transmission resonances through nanoslits drilled in a metallic membrane. *Phys. Rev. Lett.* **104**, 027401 (2010).

Acknowledgments

The research leading to these results was supported in part by the Texas Instruments Distinguished University Chair in Nanoelectronics endowment and also by the Global Frontier Program through the National Research Foundation of Korea grant NRF-2014M36AB3063708 under the Ministry of Science, ICT & Future Planning.

Author contributions

This research was planned by J.W.Y., S.H.S. and R.M. Numerical simulation was performed by J.W.Y. The authors J.W.Y., S.H.S. and R.M. discussed the results. J.W.Y., S.H.S. and R.M. wrote the manuscript.

Additional information

Competing financial interests: The authors declare no competing financial interests.

How to cite this article: Yoon, J.W., Song, S.H. & Magnusson, R. Ultrahigh-Q metallic nanocavity resonances with externally-amplified intracavity feedback. *Sci. Rep.* **4**, 7124; DOI:10.1038/srep07124 (2014).